

## Supporting Information

### **Reaction of a polydentate Cysteine-based ligand and its nickel(II) complex with electrophilic and nucleophilic methyl-transfer reagents - From S-methylation to acetyl coenzyme A synthase reactivity**

D. S. Warner, C. Limberg, Fabio J. Oldenburg and B. Braun

1. Mass spectra .....	2
2. Liquid ATR-FTIR spectra .....	6
3. NMR spectra.....	7
4. UV-vis spectrum.....	11

## 1. Mass spectra

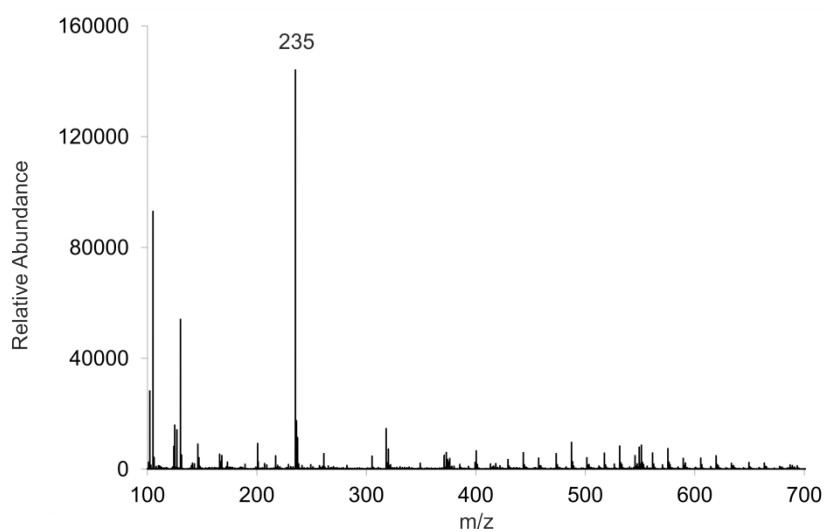


Figure S1. High-resolution ESI-MS of Me<sub>2</sub>L.

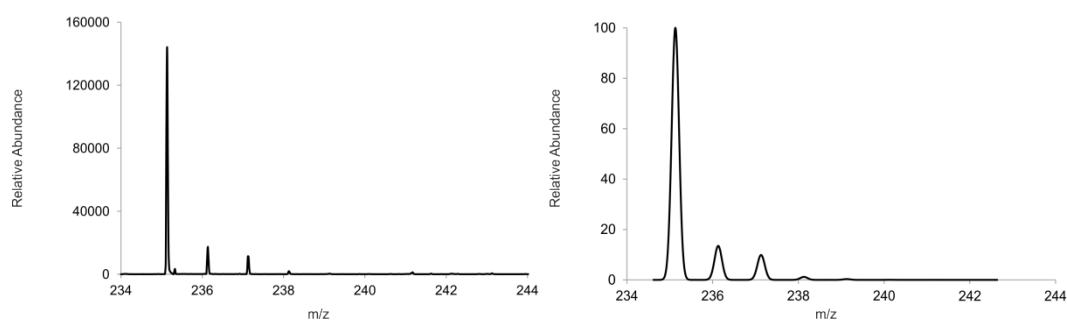


Figure S2. Measured (left) and calculated (right) isotopic pattern for the peak at  $m/z = 235.1295$  in the high-resolution ESI-MS of Me<sub>2</sub>L.

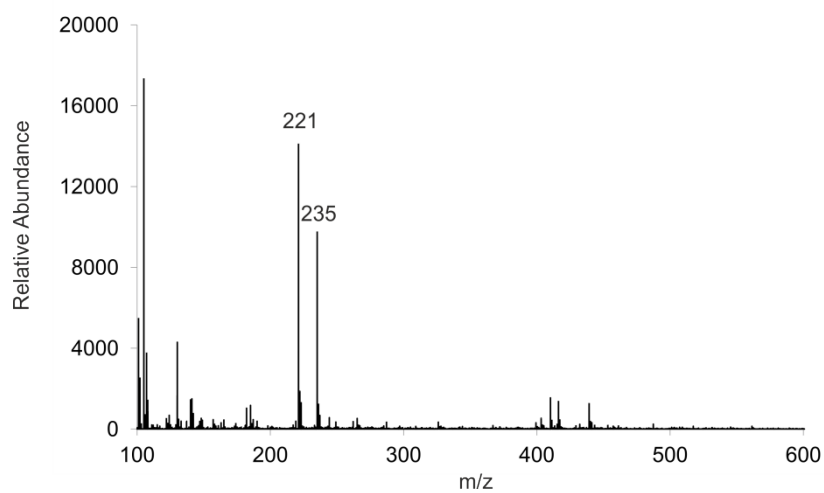


Figure S3. High-resolution ESI-MS of MeLH:  $m/z = 221$  for [MeLH]<sup>+</sup> and  $m/z = 235$  for [Me<sub>2</sub>L]<sup>+</sup>.

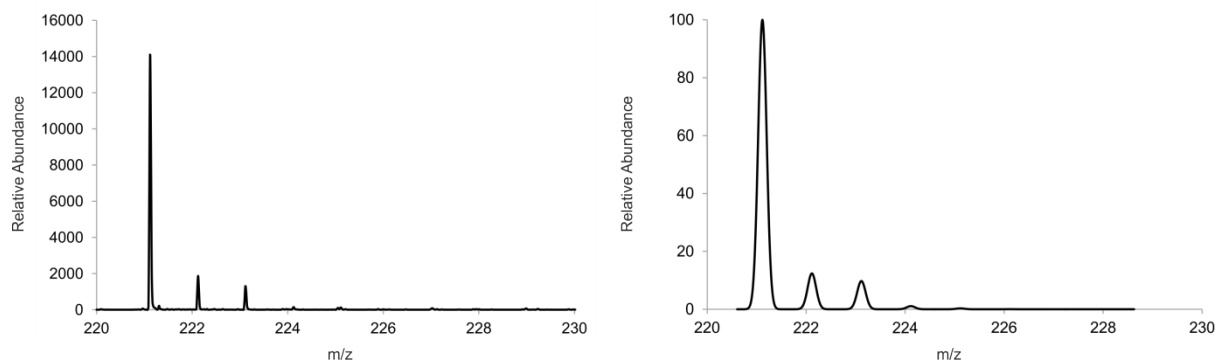


Figure S4. Measured (left) and calculated (right) isotopic pattern for the peak at  $m/z = 221.1206$  in the high-resolution ESI-MS of MeLH.

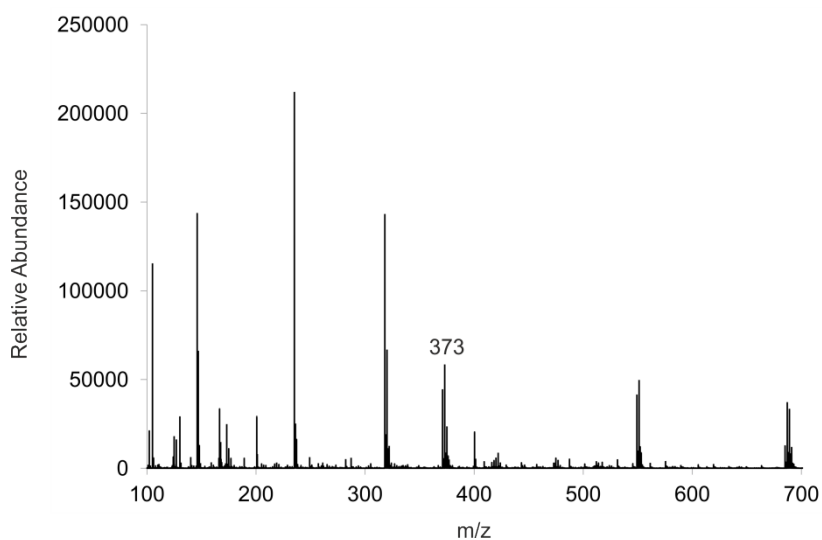


Figure S5. High-resolution ESI-MS of  $\text{Me}_2\text{LNiBr}_2$  (**2**):  $m/z = 373$  for  $[\text{Me}_2\text{LNiBr}]^+$ .

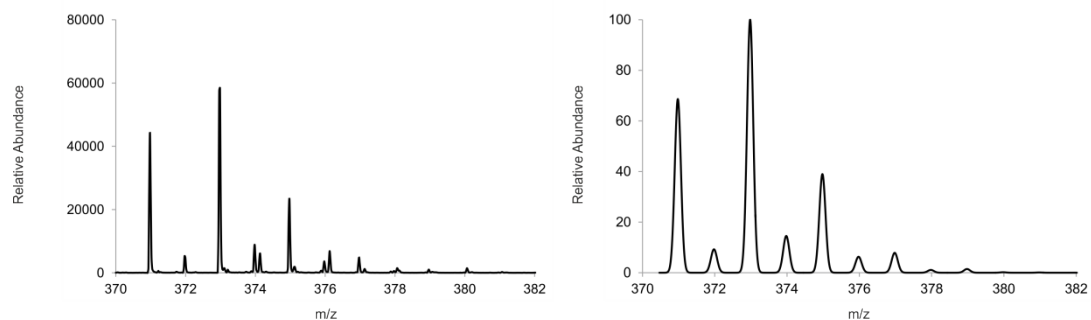


Figure S6. Measured (left) and calculated (right) isotopic pattern for the peak at  $m/z = 372.9720$  in the high-resolution ESI-MS of  $\text{Me}_2\text{LNiBr}_2$  (**2**).

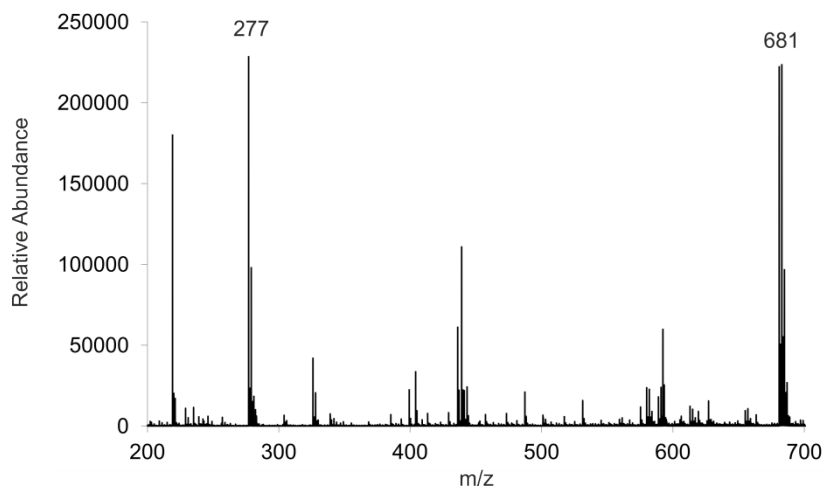


Figure S7. High-resolution ESI-MS of  $[(\text{MeNi})_3\text{I}]_2$  (**3**).

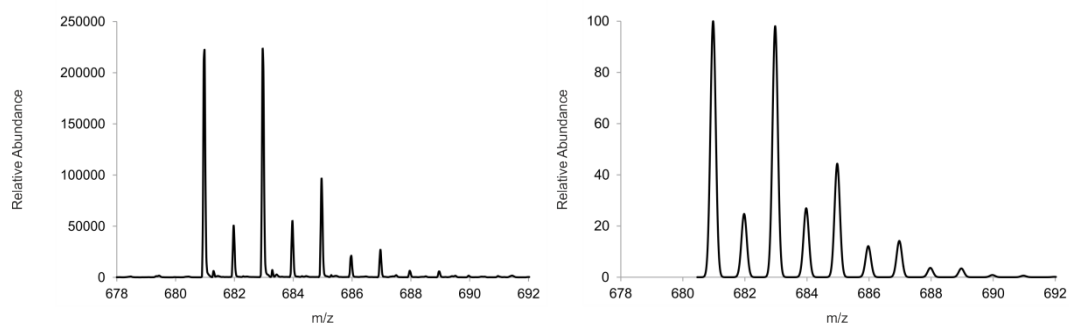


Figure S8. Measured (left) and calculated (right) isotopic pattern for the peak at  $m/z = 680.9673$  in the high-resolution ESI-MS of  $[(\text{MeNi})_3\text{I}]_2$  (**3**).

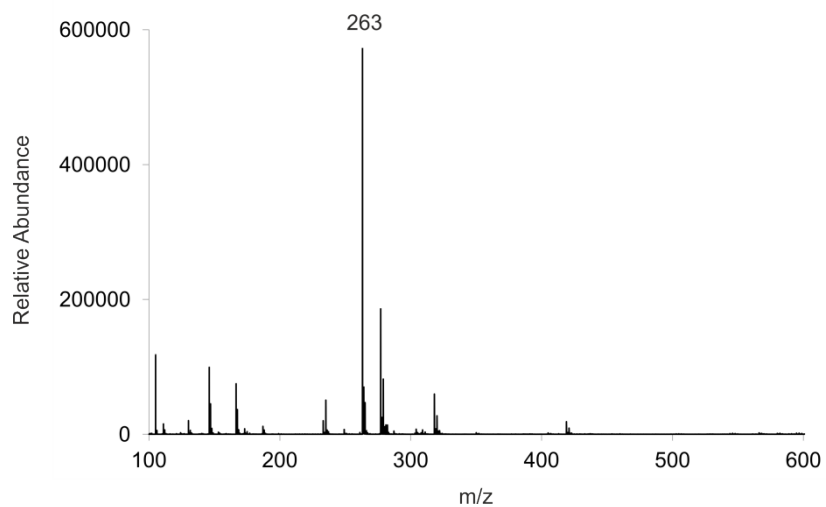


Figure S9. High-resolution ESI-MS of  $\text{MeL}(\text{CO})\text{Me}$  (**4**).

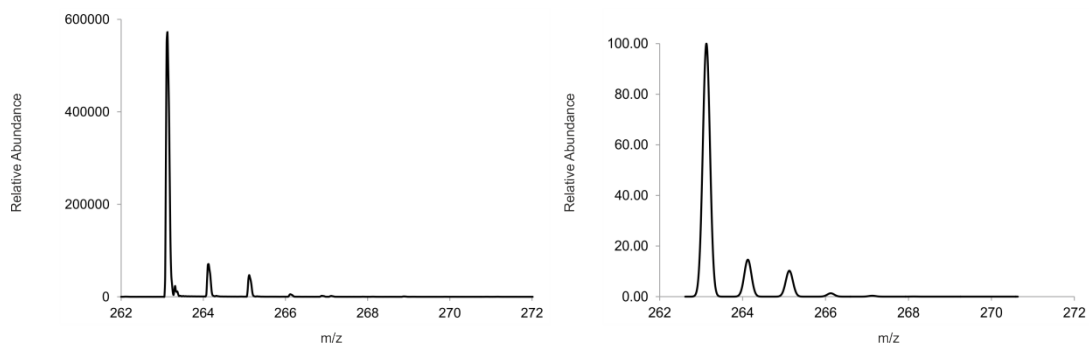


Figure S10. Measured (left) and calculated (right) isotopic pattern for the peak at  $m/z = 263.1291$  in the high-resolution ESI-MS of MeL(CO)Me (**4**).

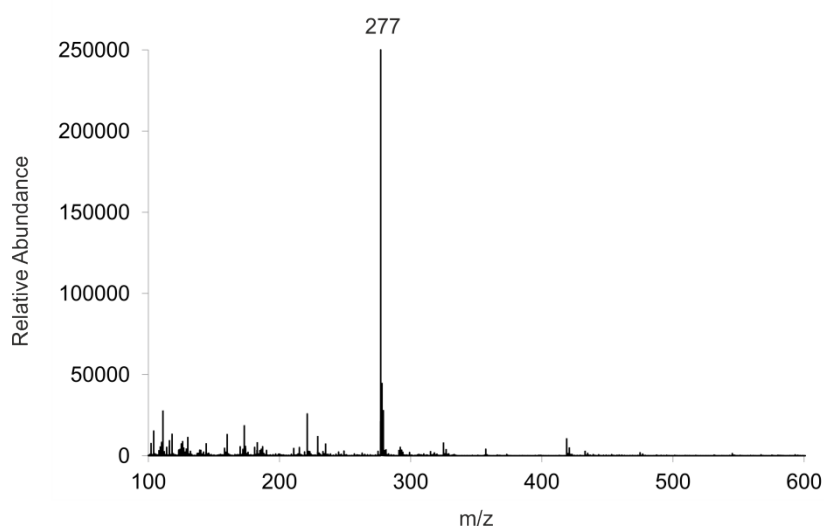


Figure S11. High-resolution ESI-MS of MeL(CO)Et (**5**).

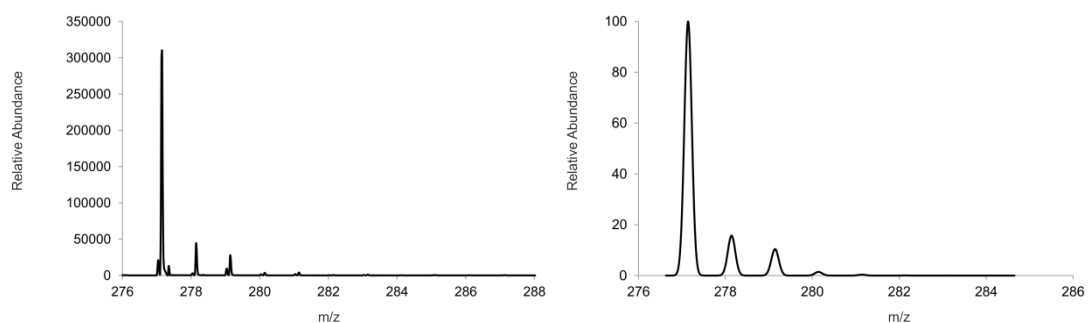


Figure S12. Measured (left) and calculated (right) isotopic pattern for the peak at  $m/z = 277.1439$  in the high-resolution ESI-MS of MeL(CO)Et (**5**).

## 2. Liquid ATR-FTIR spectra

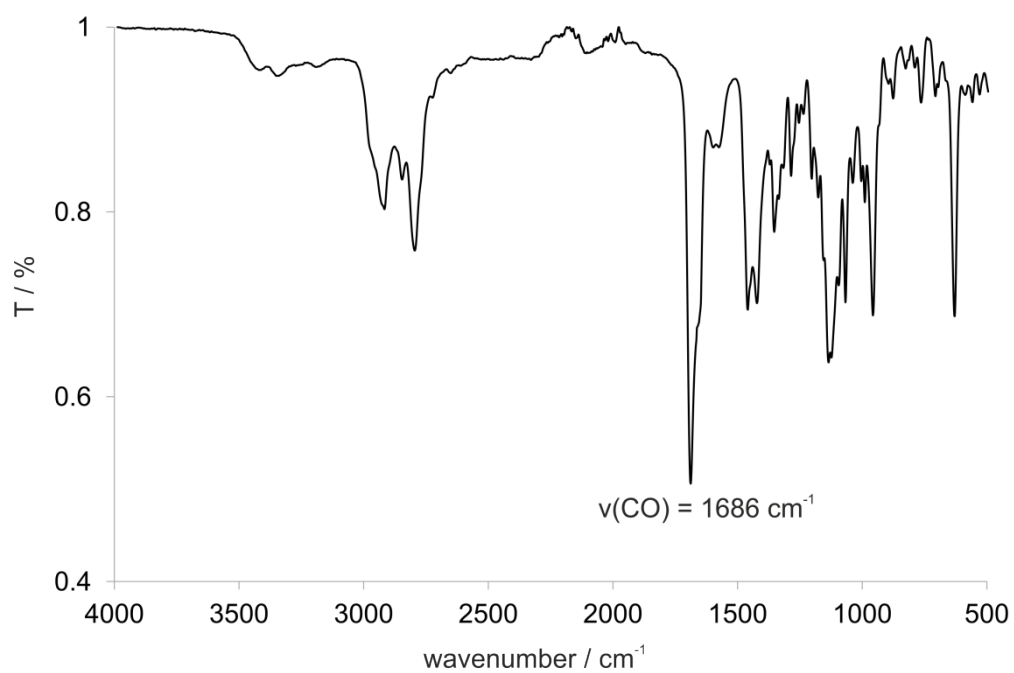


Figure S13. Liquid ATR-FTIR spectrum of MeL(CO)Me (4).

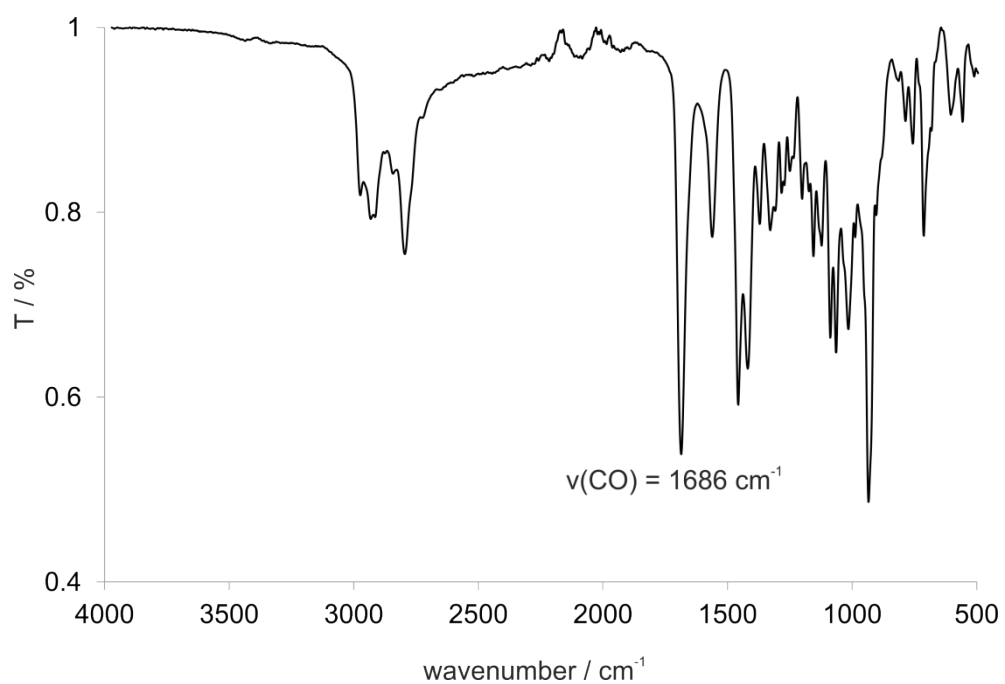


Figure S14. Liquid ATR-FTIR spectrum of MeL(CO)Et (5).

### 3. NMR spectra

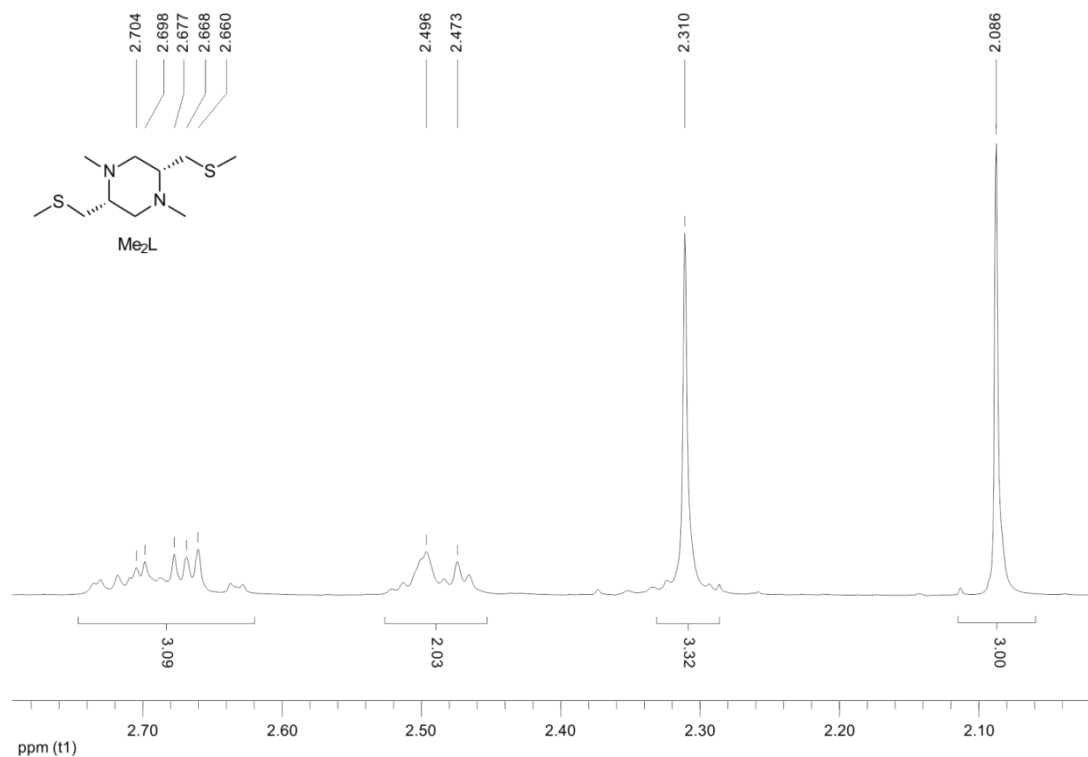


Figure S15: <sup>1</sup>H NMR (400 MHz, 297 K) spectrum of Me<sub>2</sub>L in CDCl<sub>3</sub>.

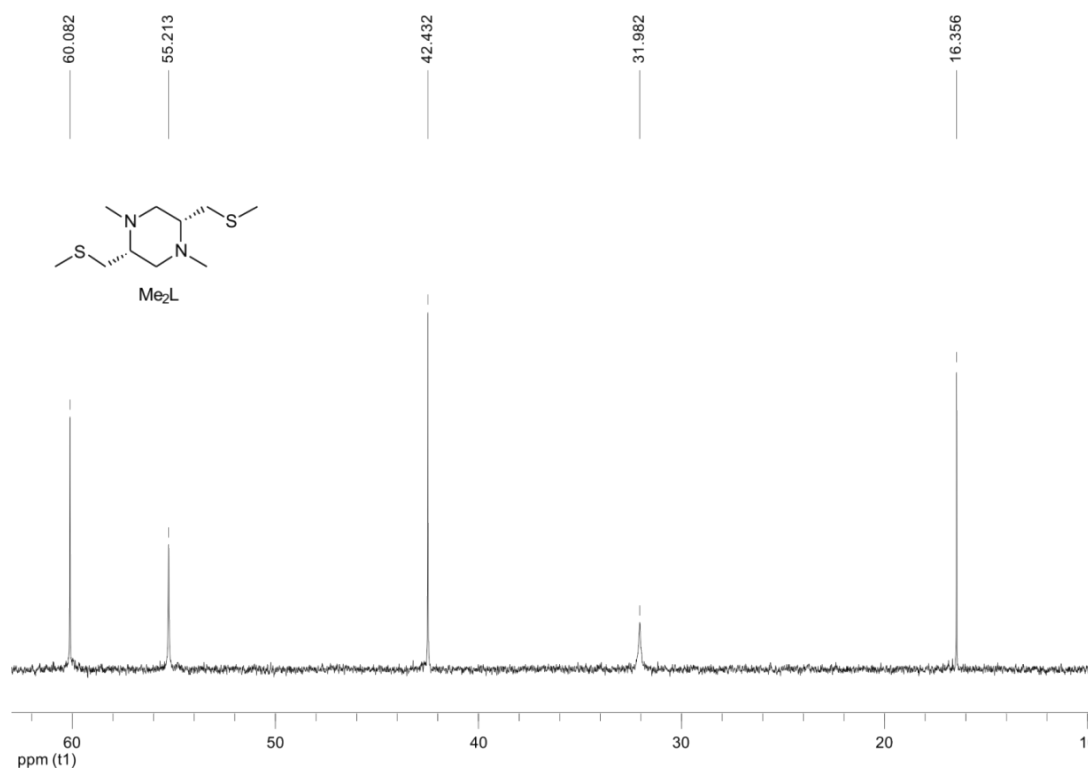


Figure S16. <sup>13</sup>C NMR (100 MHz, 297 K) spectrum of Me<sub>2</sub>L in CDCl<sub>3</sub>.

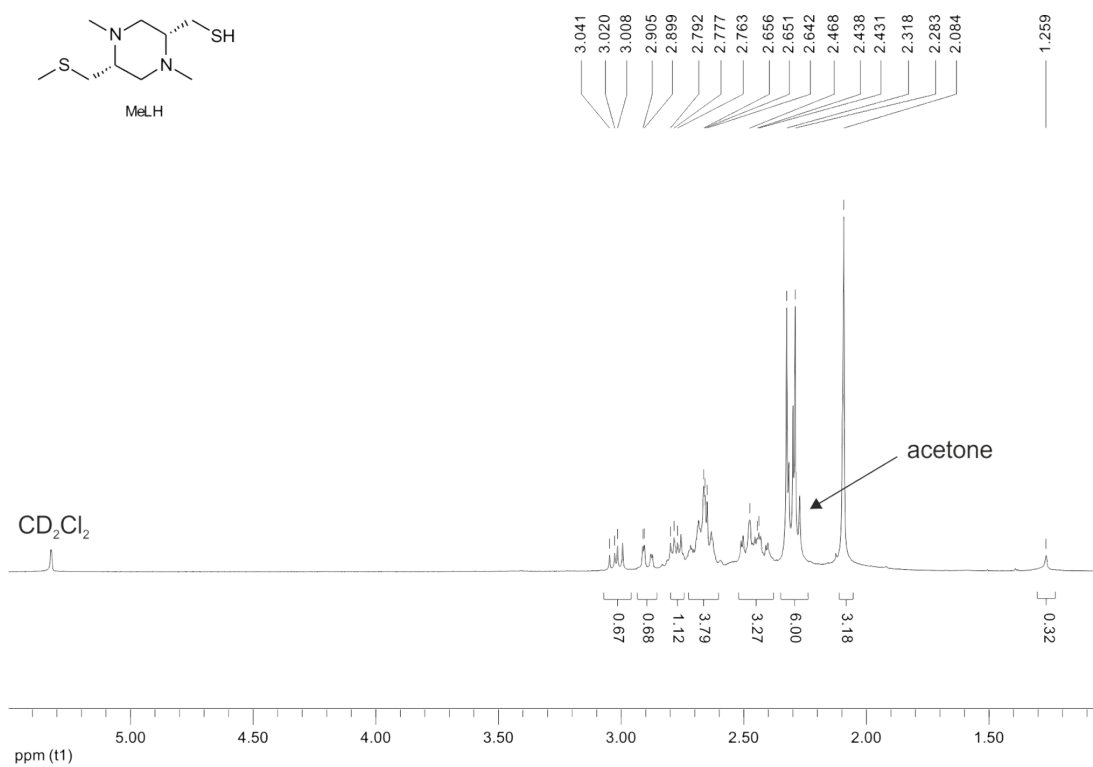


Figure S17.  $^1\text{H}$  NMR (400 MHz, 297 K) spectrum of MeLH in  $\text{CD}_2\text{Cl}_2$ .

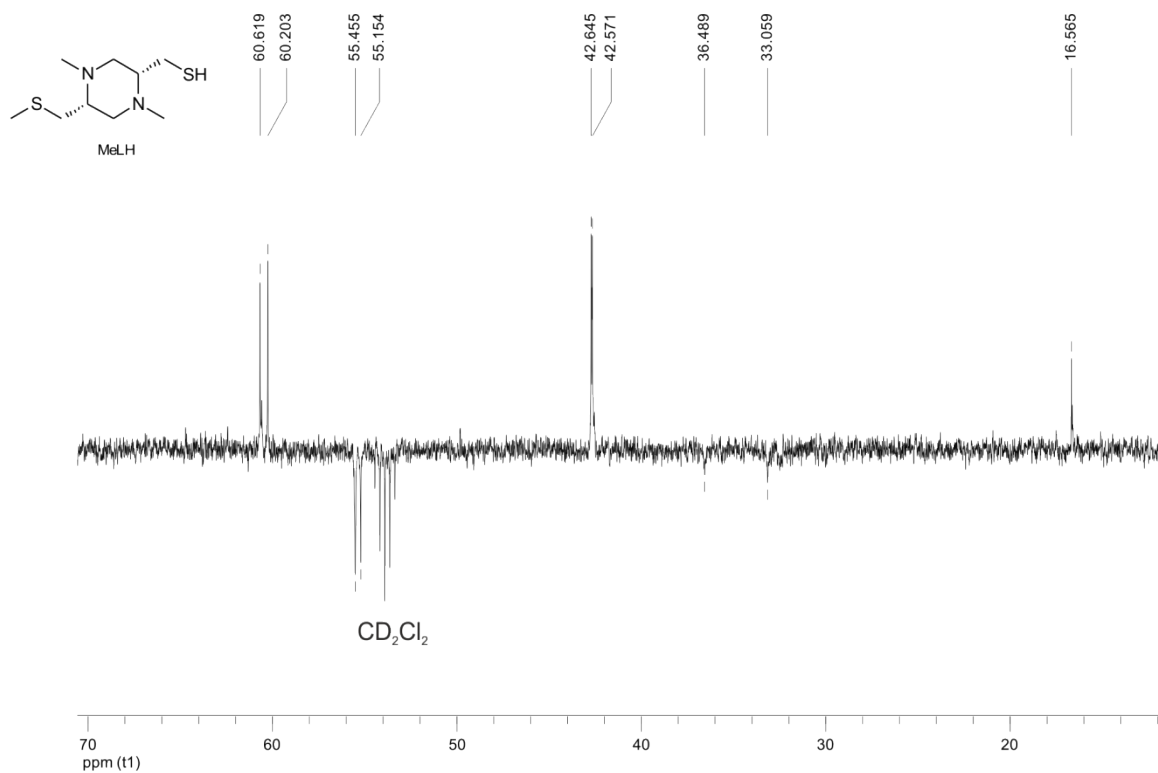


Figure S18. APT NMR (100 MHz, 297 K) spectrum of MeLH in  $\text{CD}_2\text{Cl}_2$ .

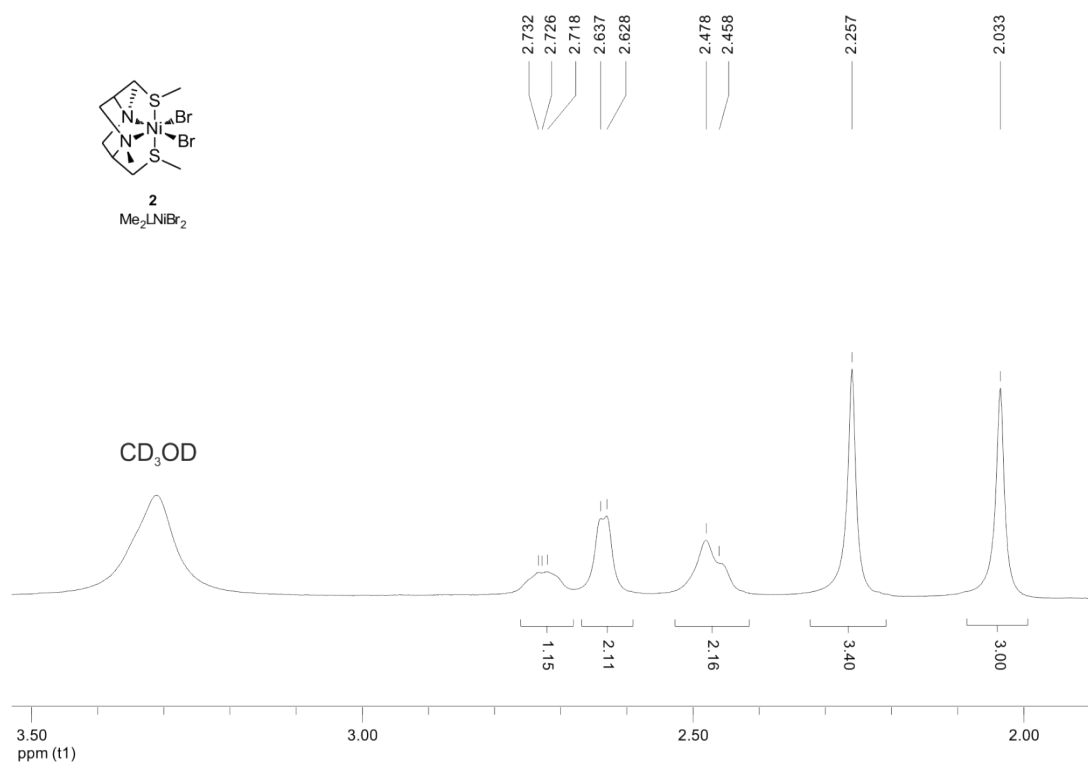


Figure S19.  $^1\text{H}$  NMR (400 MHz, 297 K) spectrum of  $\text{Me}_2\text{LNiBr}_2$  (**2**) in  $\text{CD}_3\text{OH}$ .

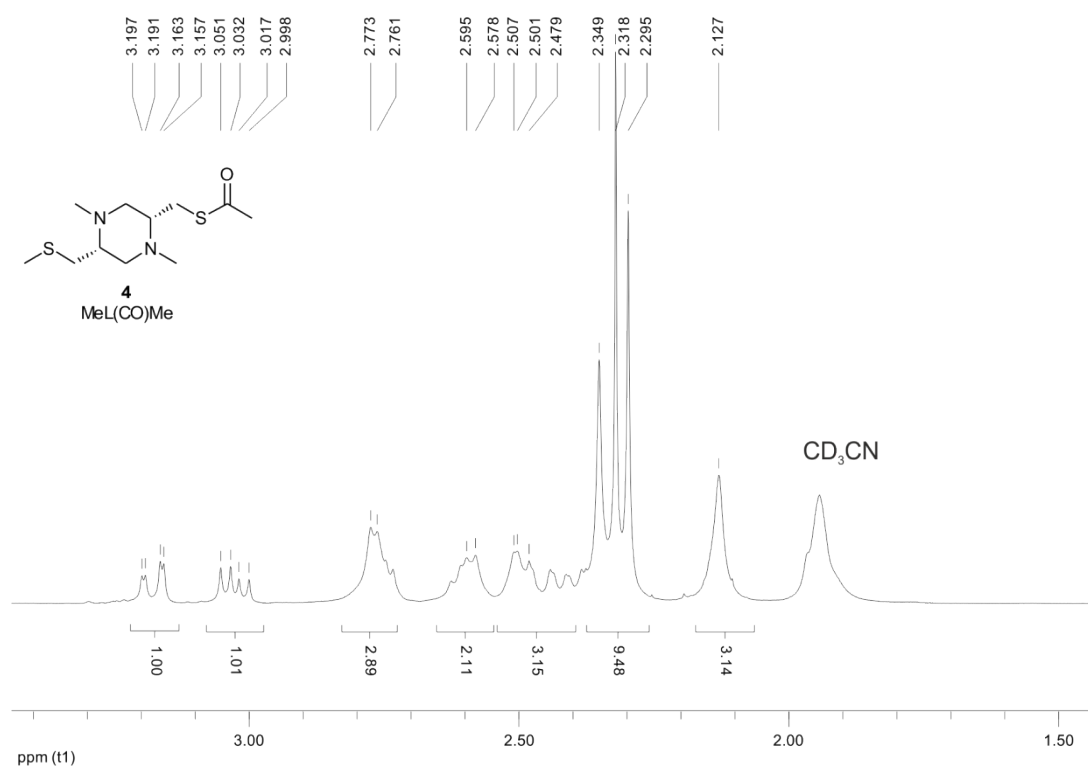


Figure S20.  $^1\text{H}$  NMR (400 MHz, 297 K) spectrum of  $\text{MeL}(\text{CO})\text{Me}$  (**4**) in  $\text{CD}_3\text{CN}$ .

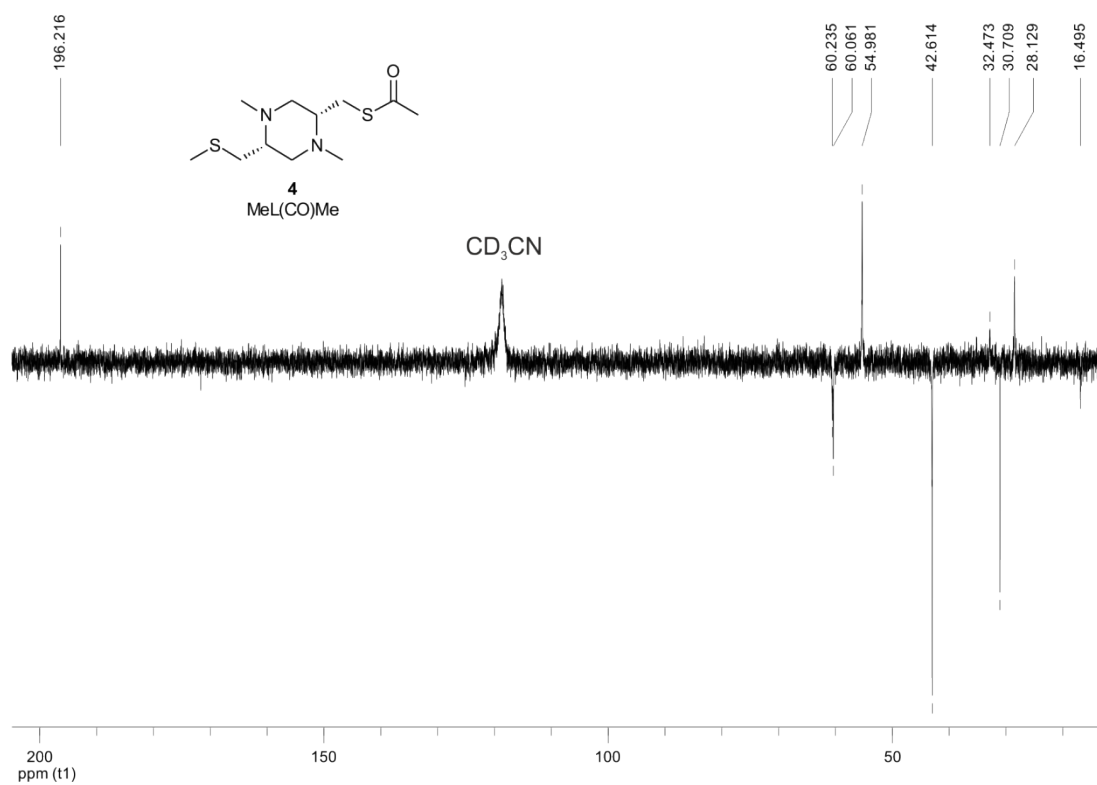


Figure S21. APT NMR (100 MHz, 297 K) spectrum of MeL(CO)Me (**4**) in CD<sub>3</sub>CN.

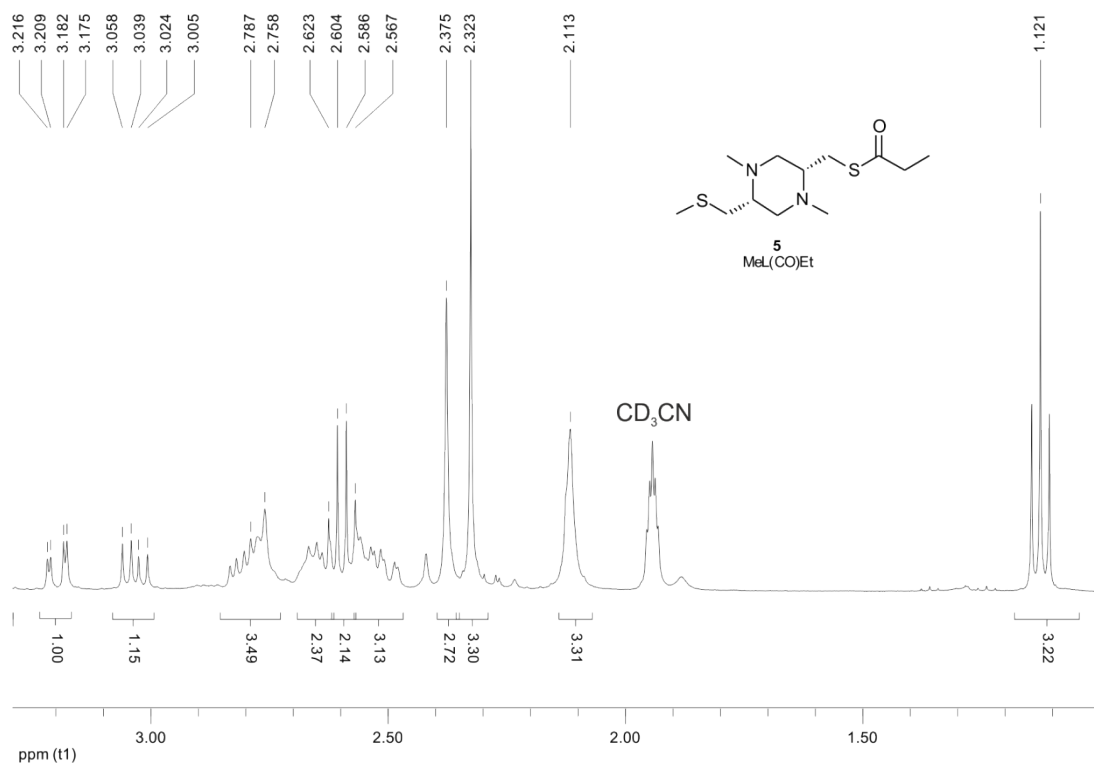


Figure S22. <sup>1</sup>H NMR (400 MHz, 297 K) spectrum of MeL(CO)Et (**5**) in CD<sub>3</sub>CN.

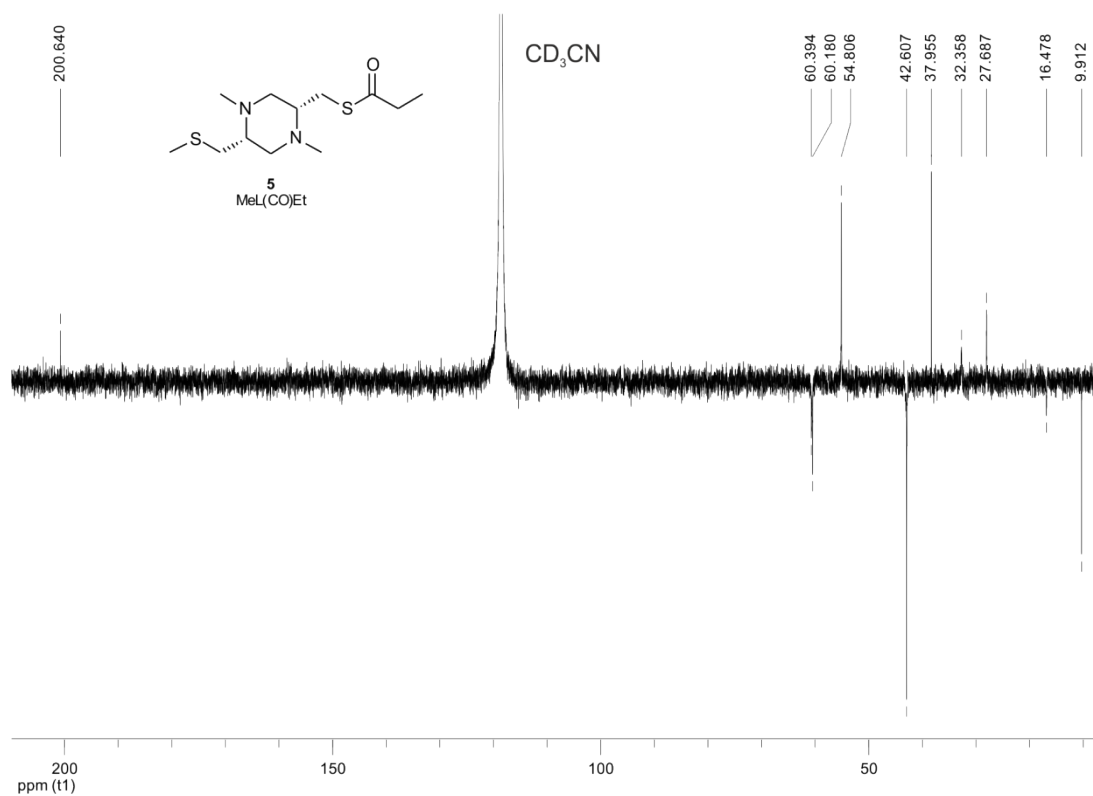


Figure S23. APT NMR (100 MHz, 297 K) spectrum of MeL(CO)Et (**5**) in CD<sub>3</sub>CN.

#### 4. UV-vis spectrum

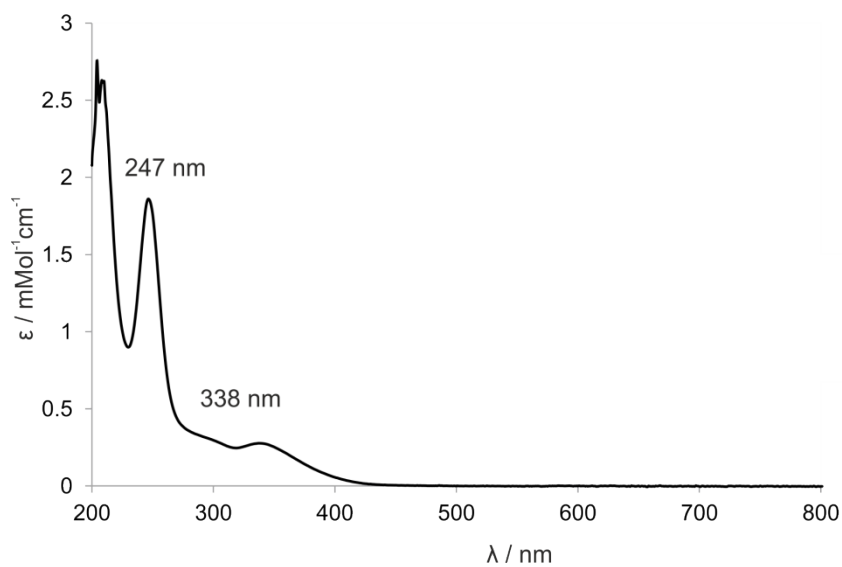


Figure S24: UV-vis spectrum of [(MeLNi)<sub>3</sub>I]<sub>2</sub> (**3**) in MeCN, 0.025 mM.